ELSEVIER

Applied Mathematical Modelling 22 (1998) 629–640

APPLIED MATHEMATICAL MODELLING

The non-Fourier effect on the fin performance under periodic thermal conditions

Jae-Yuh Lin [1]

Chang Jung University, 396 Chang Jung Rd., Sec.1, Kway Jen, Tainan, Taiwan 711, ROC

Received 17 December 1997; received in revised form 16 April 1998; accepted 2 June 1998

Abstract

This paper investigates the effect of thermal relaxation time (the non-Fourier effect) on the thermal performance of a convective fin under periodic thermal conditions. The environment heat transfer coefficient is assumed to be spatially varying. The periodic oscillation of the base temperature is considered. An efficient numerical scheme involving the hybrid application of the Laplace transform and control volume methods in conjunction with hyperbolic shape functions is used to solve the linear hyperbolic heat conduction equation. The thermal performance of the fin predicted by using the non-Fourier heat conduction model is compared with that predicted by using the Fourier model. Results show that the effects of the thermal relaxation time on the fin performance are significant for a short time after the initial transient. For the steady state, the non-Fourier effect is still great if the frequency of the temperature oscillation is high.

Keywords: Non-Fourier effect; Convective fin; Periodic heat transfer

1. Introduction

In many industrial applications such as combustion engines, electronic components and solar collectors, the analysis of fin performance under periodic thermal conditions is important. Several analytical and numerical methods [1–4] have been proposed to solve such problems. Yang [1] obtained exact analytical solution for periodic heat transfer in convective fins. Eslinger and Chung [2] presented a finite-element solution for periodic heat transfer in radiative and convective fins. Aziz and Na [3] applied the perturbation method to solve periodic heat transfer in fins with variable thermal properties. Al-Sanea and Mujahid [4] used the finite-volume numerical method to study the thermal performance of fins with time-dependent boundary conditions. The Fourier heat flux model was used to analyze the fin performance in these existing studies [1–4]. It is well known that the results obtained from the Fourier heat flux model exhibit an infinite thermal propagation speed. Despite this physically unrealistic notion of instantaneous energy diffusion, the Fourier heat flux model gives quite excellent approximations for most engineering applications. However, the classical heat conduction theory is no longer applicable when one is interested in transient heat flow in an extremely short period of time or for very low temperatures near

[1] Tel.: +886 6 278 0123; fax: +886 6 278 0111.

ISSN/98/$ – see front matter
PII: S0307-904X(98)10061-6

absolute zero. Human [5] found that the thermal propagation becomes dominant for short-pulse laser heating. Peshkov [6] experimentally determined the propagation speed of the thermal wave in helium II to be 19 m/s at a temperature of 1.4 K. Under these circumstances, the phenomena involving the finite propagation speed of the thermal wave will become dominant. With advances in microfabrication technology, the micro-heat exchanger is of interest to many engineering applications, such as the cooling of electronic chips and cryocoolers using superfluid helium II [7]. For such a situation, phenomena with the finite thermal propagation speed might be important for the thermal analysis of the extended surface in the micro heat exchanger. The existing studies [1–4] for the fin performance using the Fourier heat flux model would not be suitable for such applications. To the best of the author's knowledge, the analysis of the fin performance considering the finite thermal propagation speed has not yet been investigated in the literature.

To account for the phenomena involving the finite propagation speed of the thermal wave, the classical Fourier heat flux model should be modified. Cattaneo [8] and Vernotte [9] suggested independently a non-Fourier heat flux model in the form of

$$\tau\frac{\partial q}{\partial t}+q=-\lambda\nabla T, \tag{1}$$

where q is the heat flux, T is the temperature, λ is the thermal conductivity and τ is the relaxation time. The relaxation time τ is defined as

$$\tau=\frac{\alpha}{v^2}, \tag{2}$$

where α is the thermal diffusivity and v is the propagation speed of the thermal wave. When the relaxation time is zero, Eq. (1) is reduced to the Fourier heat flux model and the propagation speed of the thermal wave becomes infinite. Sieniutycz [10] quoted that the τ values for homogenous substances are of the order 10^{-8}–10^{-12} s. Recently, Kaminski [11] determined experimentally that the τ values for non-homogeneous inner structure materials range from 10 (for the glass ballotini) to 50 s (for the ion exchanger). The major difficulty encountered in the analysis of non-Fourier heat conduction problems is due to the numerical oscillations in the vicinity of the sharp discontinuity at the thermal wave front [12]. Chen and Lin [12] have developed an efficient numerical scheme involving the Laplace transform technique and the control volume method in conjunction with the hyperbolic shape functions to analyze non-Fourier heat conduction problems. In the present study, this hybrid numerical scheme [12] will be employed to analyze the effects of the relaxation time on the thermal performance of a convective fin under periodic heat transfer conditions.

In general, the non-Fourier effect is shown to decay quickly and both the Fourier and non-Fourier models will coincide with each other for a longer time after the initial transient [13]. However, this is not true when the heat conduction problem is subjected to an oscillatory thermal disturbance. Yuen and Lee [14] have found that the non-Fourier effect is still significant at a "long time" after the initial transient if the oscillation period of the thermal disturbance is the same order as the thermal relaxation time. Similar phenomena can also be found in the present analysis. In this study, effects of the relaxation time and the frequency of the base temperature oscillation on temperature distributions, heat transfer rates and fin efficiencies will be investigated.

2. Problem statement

The present study considers an isolated straight fin of uniform thickness b and length L, as shown in Fig. 1. The ratio of the thickness b to the length L is assumed to be very small, i.e.

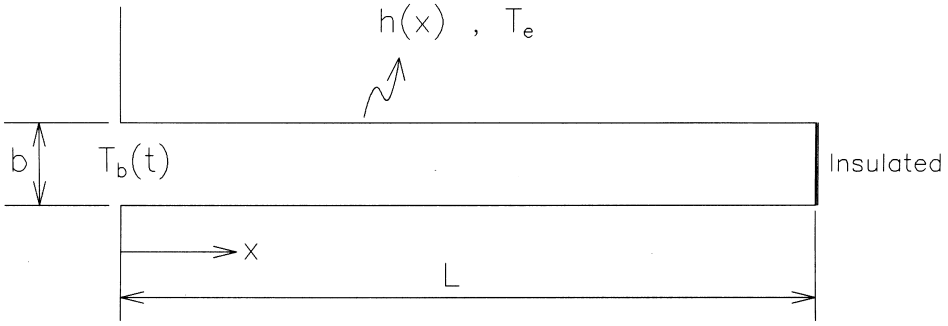

Fig. 1. Model of the fin.

$b/L \ll 1$. The fin base is attached to a surface with periodically temperature oscillation which is given as

$$T_b(t) = \overline{T}_b + (\overline{T}_b - T_{in})\, A\, \cos(\hat{\omega} t), \quad t > 0, \tag{3}$$

where $\overline{T}_b$ is the mean fin base temperature, T_{in} is the initial temperature, A is the dimensionless amplitude of the base temperature oscillation and $\hat{\omega}$ is the frequency of the base temperature oscillation. The amplitude A is a positive number less than unity. The fin tip is assumed to be kept insulated. On lateral surfaces, the fin dissipates heat to an environment at a constant temperature T_e by convection only. The radiative heat transfer is assumed to be neglected. The heat transfer coefficient h is taken to be spatially varying and is expressed as

$$h(x) = h_0\, H\left(\frac{x}{L}\right), \tag{4}$$

where h_0 is a referenced heat transfer coefficient which is defined as $h_0 = b\lambda/2L^2$ and H is a function of the space variable. The thermal conductivity λ, density ρ and specific heat c of the fin are assumed to be constant. On the assumption that $b/L, \ll 1$, the one-dimensional energy equation for the convective fin shown in Fig. 1 can be written as

$$\rho c \frac{\partial T}{\partial t} + 2\frac{h}{b}(T - T_e) = -\frac{\partial q}{\partial x}. \tag{5}$$

Eliminating $q(x,t)$ from Eqs. (1) and (5) yields the following hyperbolic heat conduction equation

$$\tau \rho c \frac{\partial^2 T}{\partial t^2} + \rho c \frac{\partial T}{\partial t} + 2\tau \frac{h}{b}\frac{\partial}{\partial t}(T - T_e) = \lambda \frac{\partial^2 T}{\partial x^2} - 2\frac{h}{b}(T - T_e). \tag{6}$$

For the convenience of numerical analysis, following dimensionless variables are introduced

$$\eta = \frac{x}{L}, \qquad \xi = \frac{\alpha t}{L^2}, \qquad \beta = \frac{\alpha \tau}{L^2}, \qquad \theta = \frac{T - T_{in}}{\overline{T}_b - T_{in}}, \qquad \omega = \frac{\hat{\omega} L}{\alpha}, \qquad \theta_e = \frac{T_e - T_{in}}{\overline{T}_b - T_{in}}. \tag{7}$$

The dimensionless governing equation can be written as

$$\beta \frac{\partial^2 \theta}{\partial \xi^2} + (1 + \beta H)\frac{\partial \theta}{\partial \xi} = \frac{\partial^2 \theta}{\partial \eta^2} - H\theta + H\theta_e. \tag{8}$$

The dimensionless boundary conditions are

$$\theta = 1 + A\, \cos(\omega \xi) \quad \text{at } \eta = 0 \tag{9a}$$

and

$$\frac{\partial\theta}{\partial\eta}=0 \quad \text{at } \eta=1. \tag{9b}$$

The dimensionless initial condition is

$$\theta=\frac{\partial\theta}{\partial\xi}=0 \quad \text{for } \xi=0. \tag{10}$$

3. Numerical analysis

To remove the ξ-dependent terms, taking the Laplace transform of Eqs. (8)–(10) with respect to the ξ variable gives

$$\frac{\mathrm{d}^2\tilde{\theta}}{\mathrm{d}\eta^2}-(\beta s^2+s+\beta Hs+H)\tilde{\theta}+\frac{1}{s}H\theta_{\mathrm{e}}=0, \tag{11a}$$

$$\tilde{\theta}=\frac{1}{s}+A\frac{s}{s^2+\omega^2} \quad \text{at } \eta=0, \tag{11b}$$

$$\frac{\mathrm{d}\tilde{\theta}}{\mathrm{d}\eta}=0 \quad \text{at } \eta=1, \tag{11c}$$

where s is the Laplace transform parameter and $\tilde{\theta}$ is the Laplace transform of the dimensionless temperature θ and is defined as

$$\tilde{\theta}(\eta,s)=\int_0^\infty \mathrm{e}^{-s\xi}\theta(\eta,\xi)\,\mathrm{d}\xi. \tag{12}$$

Subsequently, the control volume formulation is used to discretize Eqs. (11a) and (11b). Integration of Eq. (11a) over the control volume $[\eta_i-\ell/2,\eta_i+\ell/2]$ for the ith interior node can be written as [12].

$$\left.\frac{\mathrm{d}\tilde{\theta}}{\mathrm{d}\eta}\right|_{\eta_i+\ell/2}-\left.\frac{\mathrm{d}\tilde{\theta}}{\mathrm{d}\eta}\right|_{\eta_i-\ell/2}-\int_{\eta_i-\ell/2}^{\eta_i+\ell/2}(\beta s^2+s+\beta Hs+H)\tilde{\theta}\,\mathrm{d}\eta=-\frac{1}{s}\theta_{\mathrm{e}}\int_{\eta_i-\ell/2}^{\eta_i+\ell/2}H\,\mathrm{d}\eta, \tag{13}$$

where ℓ is the distance between two nodes.

In each control volume, the transformed temperature $\tilde{\theta}(\eta,s)$ should be approximated in terms of the nodal temperatures and suitable shape functions. As illustrated by Chen and Lin [12], the use of the hyperbolic shape functions can accurately solve the hyperbolic heat conduction problems. Thus, in the present study, the transformed temperatures are approximated by [12]

$$\tilde{\theta}(\eta,s)=\frac{1}{\sinh(\mu\ell)}[\sinh(\mu(\eta_i-\eta))\tilde{\theta}_{i-1}+\sinh(\mu(\eta-\eta_i+\ell))\tilde{\theta}_i] \quad \text{for } \eta\in[\eta_i-\ell,\eta_i] \tag{14a}$$

and

$$\tilde{\theta}(\eta,s)=\frac{1}{\sinh(\mu\ell)}[\sinh(\mu(\eta_i+\ell-\eta))\tilde{\theta}_i+\sinh(\mu(\eta-\eta_i))\tilde{\theta}_{i+1}] \quad \text{for } \eta\in[\eta_i,\eta_i+\ell], \tag{14b}$$

where $\mu=(\beta s^2+s)^{1/2}$.

Substituting Eqs. (14a) and (14b) into Eq. (13) leads to the following algebraic equation for the ith interior node:

$$d_i\tilde{\theta}_{i-1} + e_i\tilde{\theta}_i + f_i\tilde{\theta}_{i+1} = g_i \quad \text{for } i = 2, 3, \ldots, n-1, \tag{15}$$

where

$$d_i = \mu - (\beta s + 1)\int_{\eta_i-\ell/2}^{\eta_i} [H\ \sinh(\mu(\eta_i - \eta))]\,\mathrm{d}\eta, \tag{16a}$$

$$e_i = -2\mu\ \cosh(\mu\ell) - (\beta s + 1)\left\{\int_{\eta_i-\ell/2}^{\eta_i} [H\ \sinh(\mu(\eta - \eta_i + \ell))]\,\mathrm{d}\eta + \int_{\eta_i}^{\eta_i+\ell/2} [H\ \sinh(\mu(\eta_i - \eta + \ell))]\,\mathrm{d}\eta\right\}, \tag{16b}$$

$$f_i = \mu - (\beta s + 1)\int_{\eta_i}^{\eta_i+\ell/2} [H\ \sinh(\mu(\eta - \eta_i))]\,\mathrm{d}\eta, \tag{16c}$$

$$g_i = -\sinh(\mu\ell)\frac{1}{s}\theta_{\mathrm{e}}\int_{\eta_i-\ell/2}^{\eta_i+\ell/2} H\,\mathrm{d}\eta, \tag{16d}$$

and n is the total number of nodes.

The algebraic equation for the node at the insulated boundary $\eta = 1$ can be obtained by integrating Eq. (11a) over the control volume $[1 - \ell/2, 1]$ in conjunction with Eqs. (14a) and (14b) and is given by

$$d_n\tilde{\theta}_{n-1} + e_n\tilde{\theta}_n = g_n, \tag{17}$$

where

$$d_n = \mu - (\beta s + 1)\int_{1-\ell/2}^{1} [H\ \sinh(\mu(1 - \eta))]\,\mathrm{d}\eta, \tag{18a}$$

$$e_n = -\mu\ \cosh(\mu\ell) - (\beta s + 1)\int_{1-\ell/2}^{1} [H\ \sinh(\mu(\eta - 1 + \ell))]\,\mathrm{d}\eta, \tag{18b}$$

$$g_n = -\sinh(\mu\ell)\frac{1}{s}\,\theta_{\mathrm{e}}\int_{1-\ell/2}^{1} H\,\mathrm{d}\eta. \tag{18c}$$

The dimensionless temperature distribution in the convective fin can be determined by solving Eqs. (11b), (15) and (17). However, to analyze the fin efficiency, the dimensionless heat transfer

rate R should be determined. Once the heat transfer rate R is determined, the instantaneous fin efficiency at any specified time can be given by

$$E = R/\left[(\theta_b - \theta_e)\int_0^1 H(\eta)\,d\eta\right]. \tag{19}$$

Eq. (19) is defined as the ratio of the actual heat transfer rate to the ideal heat transfer rate when the entire fin surfaces are at the base temperature. It is obvious that the heat transfer rate R cannot be readily determined by substituting the obtained temperature distribution into the non-Fourier heat flux model, Eq. (1). Thus a further treatment is required to determine the heat transfer rate.

Integrating Eq. (11a) over the control volume [0, $\ell/2$] can yield

$$\left.\frac{d\tilde{\theta}}{d\eta}\right|_{\ell/2} - \left.\frac{d\tilde{\theta}}{d\eta}\right|_0 - \int_0^{\ell/2}(\beta s^2 + s + \beta H s + H)\tilde{\theta}\,d\eta = -\frac{1}{s}\,\theta_e\int_0^{\ell/2} H\,d\eta. \tag{20}$$

Introducing the dimensionless variables defined in Eq. (7) into Eq. (1) and then taking the Laplace transform of the dimensionless form of Eq. (1), the derivative term $d\tilde{\theta}/d\eta\big|_0$ in Eq. (20) can be written as

$$\left.\frac{d\tilde{\theta}}{d\eta}\right|_0 = -(\beta s + 1)\tilde{R}. \tag{21}$$

Substituting Eqs. (11b), (14a), (14b) and (21) into Eq. (20) can yield

$$e_1\tilde{R} + f_1\tilde{\theta}_2 = g_1, \tag{22}$$

where

$$e_1 = (\beta s + 1)\,\sinh(\mu\ell), \tag{23a}$$

$$f_1 = \mu - (\beta s + 1)\int_0^{l/2}[H\,\sinh(\mu\eta)]\,d\eta \tag{23b}$$

and

$$g_1 = \left\{\mu\,\cosh(\mu\ell) + (\beta s + 1)\int_0^{\ell/2}[H\,\sinh(\mu(\ell - \eta))]\,d\eta\right\}\left(\frac{1}{s} + A\frac{s}{s^2 + \omega^2}\right) - \sinh(\mu\ell)\frac{1}{s}\,\theta_e\int_0^{\ell/2} H\,d\eta. \tag{23c}$$

The arrangement of Eqs. (15), (17) and (22) yields the following vector–matrix equation:

$$[\boldsymbol{K}]\{\tilde{\boldsymbol{X}}\} = \{\boldsymbol{B}\}, \tag{24}$$

where $[\boldsymbol{K}]$ is an $(n \times n)$ tridiagonal matrix with complex numbers, $\{\tilde{\boldsymbol{X}}\}$ is an $(n \times 1)$ vector representing the unknown transformed variables and is expressed as

$$\{\tilde{\boldsymbol{X}}\} = \{\tilde{\boldsymbol{R}}\ \tilde{\theta}_2\ \tilde{\theta}_3 \ldots \tilde{\theta}_{n-1}\ \tilde{\theta}_n\}^T \tag{25}$$

and $\{\boldsymbol{B}\}$ is an $(n \times 1)$ vector representing the forcing terms. The dimensionless heat transfer rate R and nodal temperature θ_i can be determined by using the Gaussian elimination algorithm and the numerical inversion of the Laplace transform [15].

4. Results and discussion

In the following computations, the distance between two nodes $\ell = 0.01$ is taken. Due to the application of the Laplace transform technique, it is not required to take time steps to determine the unknown temperature and heat transfer rate at any specific time. For the illustration of numerical analysis, the present study assumes that the heat transfer coefficient function H is an exponential function of the dimensionless space variable and is expressed as

$$H(\eta) = \exp(\eta). \tag{26}$$

The value of A is taken as $A = 0.5$. The dimensionless environment temperature is taken as $\theta_e = 0.1$.

Fig. 2 shows the temperature distributions for various values of β at $\xi = 0.5$. It can be found that the thermal wave travels with a longer distance for a smaller value of β. This phenomenon can be explained by observing the definition of the thermal relaxation time as shown in Eq. (2) which states that a smaller value of the relaxation time implies a faster propagation speed of the thermal wave. The distance x_p that the thermal wave propagates at a specific time t_P can be determined by

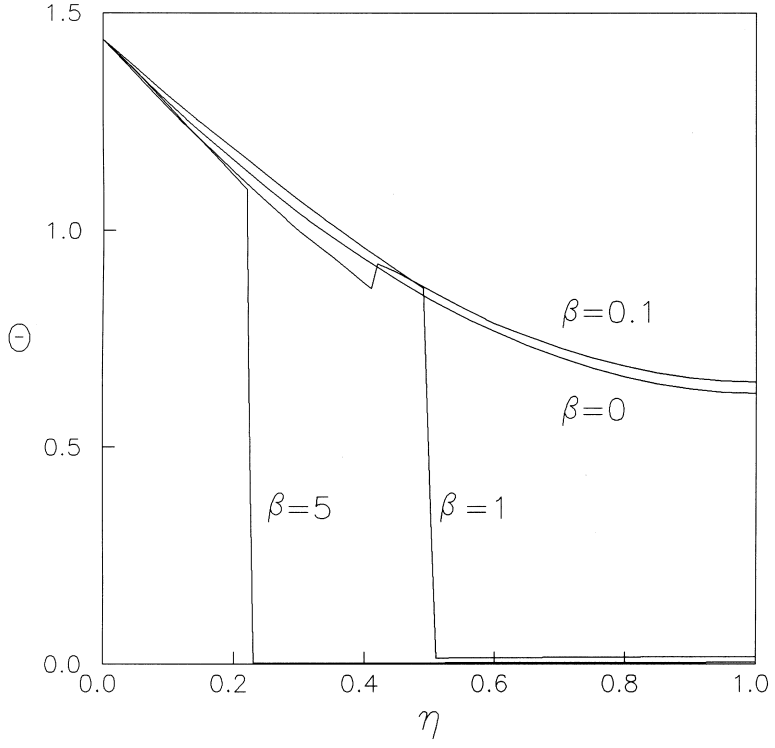

Fig. 2. Temperature distributions for various values of β ($\omega = 1$ and $\xi = 0.5$).

$$x_p = \int_0^{t_p} v \, dt = v t_p, \tag{27}$$

where v is the propagation speed of the thermal wave and is assumed to be constant. Using Eqs. (2), (7) and (27) can be rewritten as

$$\eta_p = \frac{\xi_p}{\sqrt{\beta}}. \tag{28}$$

The thermal propagation speed for $\beta = 0$ becomes infinity and no jump discontinuity takes place. For the case of $\beta = 0.1$, the original thermal wave has reached the fin tip and was reflected from the insulated tip and then interacted with the new thermal wave from the base at $\eta = 0.42$. For $\beta = 1$, the thermal wave arrives at $\eta = 0.5$ and the region $\eta > 0.5$ is not influenced by the base temperature oscillation, but the convective heat transfer from the environment. For $\beta = 5$, the jump discontinuity takes place at $\eta = 0.23$. Fig. 3 shows the temperature distributions for various values of ω when $\beta = 1$. It can be found that the oscillation frequency does not affect the location of the jump discontinuity. This can be explained by Eq. (28). The distance that the thermal wave propagates depends only on the values of ξ and β.

Fig. 4 investigates the effect of the relaxation time β on the fin tip temperature variation, heat transfer rate and instantaneous fin efficiency. It can be found that for the short time after the initial transient, remarkable jump discontinuity can be observed because of the finite propagation speed of the thermal wave. The strength of the discontinuity reduces with time due to heat diffusion. The non-Fourier effect is still significant when the fin performance reaches the steady state (for $\xi > 8$). A larger value of β implies a stronger non-Fourier effect. This is quite different from

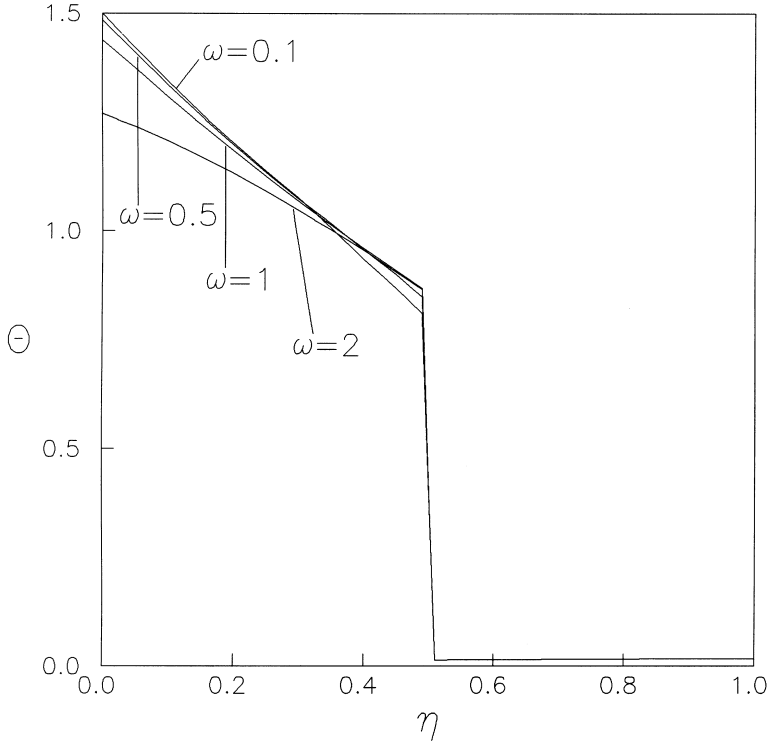

Fig. 3. Temperature distributions for various values of ω ($\beta = 1$ and $\xi = 0.5$).

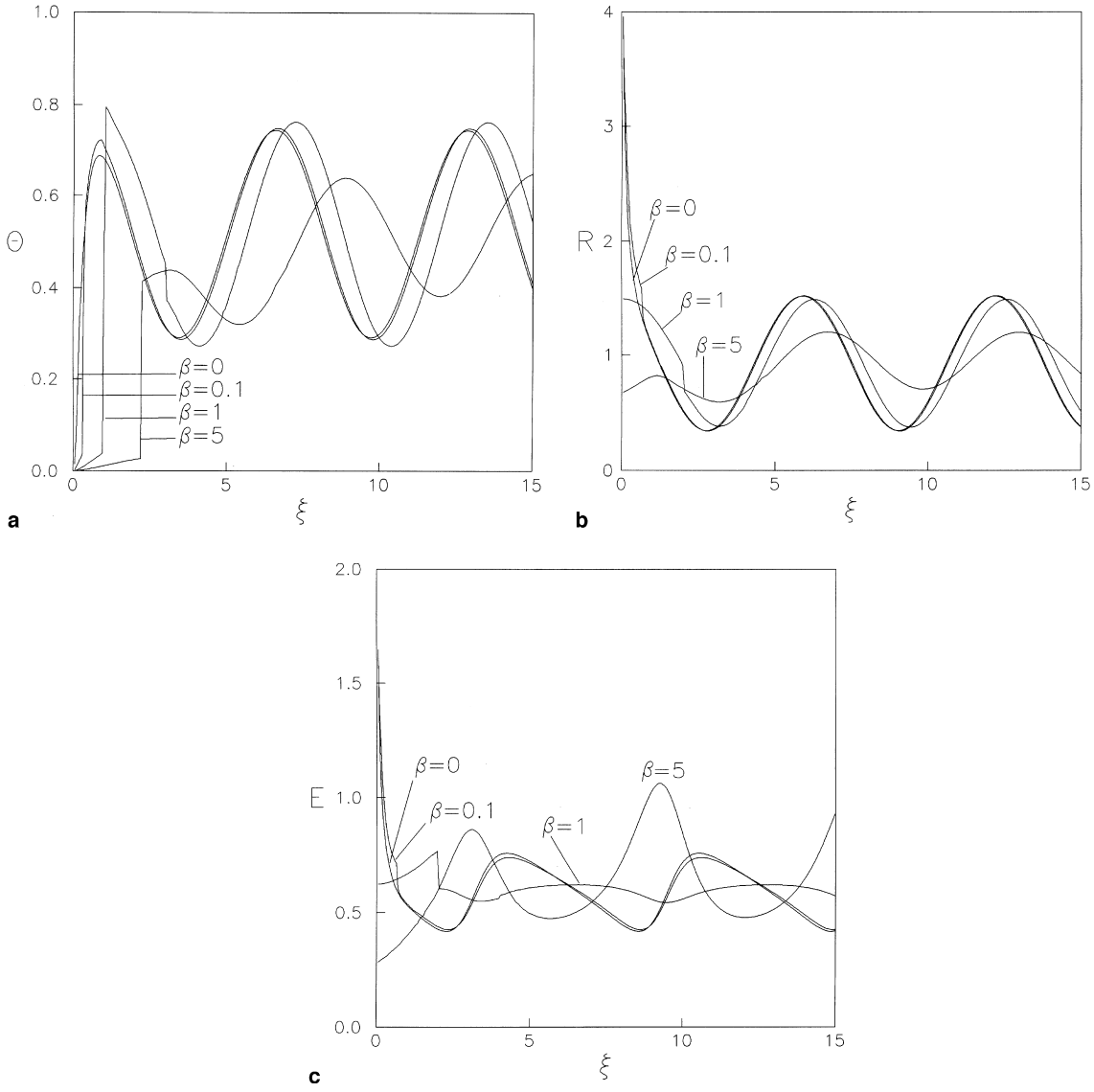

Fig. 4. Effects of parameter β on the fin performance ($\omega = 1$): (a) fin tip temperature variation; (b) heat transfer rate; (c) instantaneous fin efficiency.

most of the non-Fourier heat transfer analysis which stated that the non-Fourier heat flux model will coincide with the Fourier heat flux model for a longer time after the initial transient [13]. The phase difference between the Fourier and non-Fourier results increases when the value of β is increased. This is due to the fact that the heat flow does not start instantaneously, but grows gradually with a relaxation time after applying a temperature gradient. As shown in Fig. 4(b), the amplitude of the heat transfer rate variation decreases when the value of β is increased. According to Eq. (19), the phase difference between the heat transfer rate and the base temperature oscillation will affect the fin efficiency. Since this phase difference varies with the value of β, it can be found from Fig. 4(c) that the amplitude of the instantaneous fin efficiency variation in the steady state decreases and then increases with increasing the value of β. A physically unrealistic phenomenon due to the assumption of instantaneous energy diffusion can be observed in Fig. 4(b).

The heat transfer rate for the Fourier heat flux model ($\beta = 0$) will approach infinity in the limit $\xi \to 0$.

Instead of the instantaneous fin efficiency, the average fin efficiency will be a more meaningful quantity in the evaluation of fin performance. When the fin performance has become steady state, the average fin efficiency over a complete cycle can be evaluated in the following

$$E_{\mathrm{av}} = \frac{\omega}{2\pi} \int_0^{\omega/2\pi} E \, \mathrm{d}\xi. \tag{29}$$

Fig. 5 presents the effects of the relaxation time β and the frequency of the base temperature oscillation ω on the average fin efficiency. It can be found that for $\beta \ll 1$ the average fin efficiency decreases when the value of ω is increased. This tendency is similar to the conventional fin analysis using the Fourier heat flux model [1–4]. However, for a large value of β, the average fin efficiency increases when the value of ω is increased. It is different from the conventional fin analysis [1–4]. For a specific value of ω, as the value of β is increased, the average fin efficiency will decrease to a minimum value and then increase. For the case of $\omega = 0.01$, the thermal relaxation time has little effect on the average fin efficiency. This means that the Fourier heat flux model is suitable for the analysis of fin performance when the frequency of the base temperature oscillation is very low. As the value of ω is increased, the difference of average fin efficiency between the Fourier model ($\beta = 0$) and the non-Fourier model will increase. It can be concluded that the non-Fourier effect should be considered in the thermal analysis of a fin performance when the period of the base temperature oscillation $2\pi/\omega$ is less than or equal to the thermal relaxation time β.

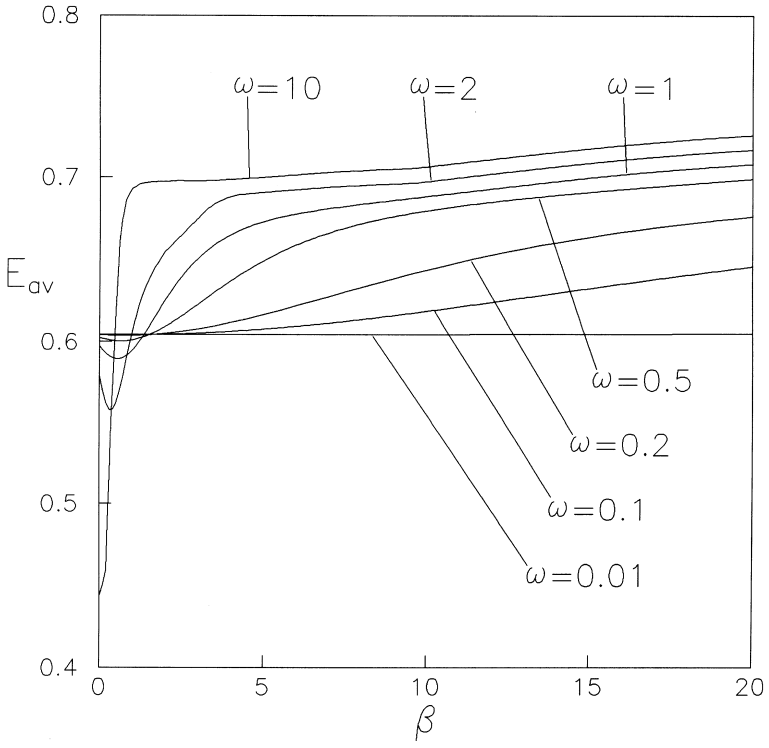

Fig. 5. Effects of parameters β and ω on the average fin efficiency.

5. Conclusion

The non-Fourier effect on the thermal performance of a convective fin under periodic thermal conditions is investigated numerically by using a hybrid numerical method combining the Laplace transform and control volume methods. It is found from the present study that the hybrid Laplace transform method in conjunction with the hyperbolic shape functions solves the present hyperbolic heat conduction problems accurately. The non-Fourier effect is found to be significant for a short time after the initial transient. Moreover, the effect of the relaxation time is still significant when the fin performance reaches the steady state if the frequency of base temperature oscillation is high. This means that the conventional fin analysis using the Fourier heat flux model will give rise to great errors when a fin is modelled under a periodic thermal condition whose period of oscillation is less than or equal to the order of the thermal relaxation time.

Nomenclature

A amplitude of temperature oscillation
b thickness of fin
c specific heat
E instantaneous fin efficiency
E_{av} average fin efficiency
H dimensionless heat transfer coefficient function
h heat transfer coefficient
h_0 referenced heat transfer coefficient
L length of fin
ℓ distance between two nodes
n total number of nodes
Q dimensionless heat flux
q heat flux
R dimensionless heat transfer rate
s Laplace transform parameter
T temperature
T_{in} initial temperature
t time
v propagation speed of thermal wave
x space coordinate

Greek symbols

α thermal diffusivity
β dimensionless relaxation time
η dimensionless space coordinate
λ thermal conductivity
μ $(\beta s^2 + s)^{1/2}$
ω dimensionless frequency of base temperature oscillation
$\hat{\omega}$ frequency of base temperature oscillation
θ dimensionless temperature
ρ density
τ relaxation time
ξ dimensionless time

Superscripts

− mean temperature

∼ Laplace transformed variable

Subscripts

b base

e environment

References

[1] Y.W. Yang, Periodic heat transfer in straight fins, J. Heat Transfer 94 (1972) 310–314.

[2] R.G. Eslinger, B.T.F. Chung, Periodic heat transfer in radiating and convecting fins or fin arrays, AIAA J. 17 (1979) 1134–1140.

[3] A. Aziz, T.Y. Na, Periodic heat transfer in fins with variable thermal parameters, Internat. J. Heat Mass Transfer 24 (1981) 1397–1404.

[4] S.A. Al-Sanea, A.A. Mujahid, A numerical study of the thermal performance of fins with time-dependent boundary conditions, including initial transient effects, Wärme-und Stoffübertragung 28 (1993) 417–424.

[5] M. Human, Non-Fourier heat transfer in laser heated metal surfaces, in: J.H. Kim et al. (Eds.), Heat Transfer: Korea–USA Seminar, 1986, pp. 521–533.

[6] V. Peshkov, Second sound in helium II, J. Phys. USSR 8 (1997) 381.

[7] P. Jiang, B. Wang, Z. Ren, Micro heat exchanger and relevant problems, J. Engineering Thermophysics 17 (1996) 328–332.

[8] C. Cattaneo, On the conduction of heat, Atti Del Seminar. Mat. Fis. Univ. Modena 3 (1948) 3.

[9] M.P. Vernotte, Paradoxes in the continuous theory of the heat equation, Compt. Rend. Acad. Sci. (Paris) 246 (1958) 3154–3155.

[10] S. Sieniutycz, The variational principle of classical type for non-coupled non-stationary irreversible transport processes with convective motion and relaxation, Internat. J. Heat Mass Transfer 20 (1977) 1221–1231.

[11] W. Kaminiski, Hyperbolic heat conduction equation for materials with a non-homogeneous structure, J. Heat Transfer 112 (1990) 555–560.

[12] H.T. Chen, J.Y. Lin, Numerical analysis for hyperbolic heat conduction, Internat. J. Heat Mass Transfer 36 (1993) 2891–2898.

[13] B. Vick, M.N. Özisik, Growth and decay of a thermal pulse predicted by the hyperbolic heat conduction equation, J. Heat Transfer 105 (1983) 902–907.

[14] W.W. Yuen, S.C. Lee, Non-Fourier heat conduction in a semi-infinite solid subjected to oscillatory surface thermal disturbances, J. Heat Transfer 111 (1989) 178–181.

[15] G. Honig, U. Hirdes, A method for the numerical inversion of Laplace transforms, J. Comput. Appl. Math 9 (1984) 113–132.